Sliding Mode Control of F-16 Longitudinal Dynamics

Sridhar Seshagiri
ECE Dept., San Diego State University
San Diego, CA 92182, USA
seshagir@engineering.sdsu.edu

Ekprasit Promtun*
Royal Thai Air Force, Thailand
promtun@rohan.sdsu.edu

Abstract— We consider the application of a conditional integrator based sliding mode control design for robust regulation of minimum-phase nonlinear systems to the control of the longitudinal flight dynamics of an F-16 aircraft. The design exploits the modal decomposition of the linearized dynamics into its short-period and phugoid approximations. The control design is based on linearization, but is implemented on the nonlinear multiple-input multiple-output longitudinal model of the F-16 aircraft. We consider model following for the angle-of-attack, with the regulation of the aircraft velocity (or the Mach-hold autopilot) as a secondary objective. It is shown through extensive simulations that the inherent robustness of the SMC design provides a convenient way to design controllers without gain scheduling, with transient performance that is far superior to that of a conventional gain-scheduled approach with integral control.

I. INTRODUCTION

The dynamic response characteristics of aircraft are highly nonlinear. Traditionally, flight control systems have been designed using mathematical models of the aircraft linearized at various flight conditions, with the controller parameters or gains "scheduled" or varied with the flight operating conditions. Various robust multivariable techniques including linear quadratic optimal control (LQR/LQG), H_∞ control, and structured singular value μ-synthesis have been employed in controller design, an excellent and exhaustive compendium of which is available in [10]. In order to guarantee stability and performance of the resulting gain-scheduled controllers, analytical frameworks of gain scheduling have been developed, including the powerful technique of linear-parameter-varying (LPV) control [4], [9], [18], [21]. Nonlinear design techniques such as dynamic inversion have been used in [1], [14], [20], while a technique that combines model inversion control with an online adaptive neural network to "robustify" the design is described in [16], and a nonlinear adaptive design based on backstepping and neural networks in [7]. A RBFNN based adaptive design with time-scale separation between the system and controller dynamics, with applications to control of both longitudinal (angle-of-attack command systems) as well as lateral (regulation of the sideslip and roll angles) is described in [23]. A succinct "industry perspective" on flight control design, including the techniques of robust control (H_∞, μ-synthesis), LPV control, dynamic inversion, adaptive control, neural networks, and more, can be found in [3].

Our interest is in the design of robust sliding mode control (SMC) for the longitudinal flight dynamics of a F-16 aircraft

that does not use gain-scheduling. The application of SMC to flight control has been pursued by several others authors, see, for example, [5], [6], [19]. Our work differs from earlier ones in that it is based on a recent technique in [17] for introducing integral action in SMC. While we design a nonlinear controller, it is still designed *based* upon plant linearization. In particular, our design exploits the modal decomposition of the linearized dynamics into its short-period and phugoid approximations. Our primary emphasis is on the transient and steady-state performance of control of the aircraft's angle of attack, with the steady-state performance and disturbance rejection of the aircraft's velocity as a (minor) secondary objective. The desired transient and steady-state specifications for the angle of attack are encapsulated in the response of a reference model, and the (SMC) controller is designed as a model-following controller. As a consequence of exploiting the modal decomposition of the aircraft dynamics, the controller has a very simple structure. It is simply a high-gain PI/PID controller with an "anti-windup" integrator, followed by saturation. This controller structure is a special case of a general design for robust output regulation for multiple-input multiple-output (MIMO) nonlinear systems transformable to the normal form, with analytical results for stability and performance described in [17]. Through simulations, we show the efficacy of the design and that it outperforms a traditional gain-scheduled controller design based on the polynomial approach to model-following design.

The rest of this paper is organized as follows. In Section 2, we describe the nonlinear mathematical aircraft model, its linearization and the decomposition of the dynamics into the short-period and phugoid modes. This section is extracted mostly from [22], with the Simulink model for simulation purposes based on [15]. Controller design is discussed in Section 3, and simulation results showing the efficacy of the design are presented in Section 4. Finally, a summary of our work and some suggestions for possible extensions are provided in Section 5.

II. 3-DOF LONGITUDINAL MODEL

Assuming no thrust-vectoring, the equations for pure longitudinal motion (pitching and translation) of a high performance aircraft can be described by the 5th order nonlinear

longitudinal state model [8], [22]

$$
\begin{aligned}
\dot{V} &= \frac{\bar{q}S\bar{c}q}{2mV}\left[C_{xq}(\alpha)\cos\alpha + C_{zq}(\alpha)\sin\alpha\right] \\
&\quad + \frac{\bar{q}S}{m}\left[C_x(\alpha,\delta_e)\cos\alpha + C_z(\alpha,\delta_e)\sin\alpha\right] \\
&\quad - g\sin(\theta-\alpha) + \frac{T}{m}\cos(\alpha) \\
\dot{\alpha} &= q\left[1 + \frac{\bar{q}S\bar{c}}{2mV^2}(C_{zq}(\alpha)\cos\alpha - C_{xq}\sin\alpha)\right] \\
&\quad + \frac{\bar{q}S}{mV}\left[C_z(\alpha,\delta_e)\cos\alpha - C_x(\alpha,\delta_e)\sin\alpha\right] \\
&\quad + \frac{g}{V}\cos(\theta-\alpha) - \frac{T}{mV}\sin(\alpha) \\
\dot{\theta} &= q \\
\dot{q} &= \frac{\bar{q}S\bar{c}q}{2I_yV}\left[\bar{c}C_{mq}(\alpha) + \Delta C_{zq}(\alpha)\right] \\
&\quad + \frac{\bar{q}S\bar{c}}{I_y}\left[C_m(\alpha,\delta_e) + \frac{\Delta}{\bar{c}}C_z(\alpha,\delta_e)\right] \\
\dot{h} &= V\sin(\theta-\alpha)
\end{aligned}
\tag{1}
$$

where V, α, θ, q and h are the aircraft's velocity, angle-of-attack, pitch attitude, pitch rate and altitude respectively, T the thrust force, δ_e the elevator angle, m the mass of the aircraft, I_y the moment of inertia about the Y-body axis, $\bar{q} = \bar{q}(h,V) = \frac{1}{2}\rho(h)V^2$ the dynamic pressure, S the wing area, Δ the distance between the reference and actual center of gravity, $C_m(\cdot)$ the pitching moment coefficient along the Y-body axis, $C_{mq}(\cdot) = \frac{\partial C_m}{\partial q}$ the variation of C_m with pitch rate, $C_x(\cdot)$ and $C_z(\cdot)$ the force coefficients along the stability X and Z axes respectively, and $C_{xq}(\cdot)$ and $C_{zq}(\cdot)$ the variations of these coefficients with the pitch rate. The system (1) can be compactly written in standard form as $\dot{x} = f(x,u)$, $y = h(x)$, where $x = [V\ \alpha\ \theta\ q\ h]^T \in R^5$ is the state vector, and $u = [T\ \delta_e]^T \in R^2$, $y = [V\ h]^T \in R^2$ are the control input and the measured "linearizing outputs" respectively. We build a Simulink model for the above longitudinal dynamics for a scaled F-16 aircraft model based on NASA Langley wind tunnel tests [11], as described in [15], [22]. Our model differs from the ones in [15], [22] primarily in that

1) We only build a 3-DOF 5th order longitudinal model (so $\beta = 0$) as opposed to the 6-DOF model for the full 12th order nonlinear state model.
2) We do not include lag effects. For example, the NASA data [11] includes a model of the F-16 afterburning turbofan engine, in which the thrust response is modeled as a first-order lag, and the lag time constant is a function of the actual engine power level, and the commanded power. The command power is related to the throttle position δ_{th}, which is taken as the input in place of the thrust T, and the inclusion of the engine model increases the system order by one. However, we include magnitude saturation in our simulation.
3) We ignore the leading flap edge deflection. The F-16 has a leading-edge flap that is automatically controlled as a function of α and Mach and responds rapidly to α changes during maneuvering (see [15] for a further discussion), and
4) We consider a smaller dynamic range for the angle of attack, $\alpha \in [-10°, 45°]$.

In particular, the model that we build corresponds to the *low fidelity* F-16 longitudinal model in [15], and to the longitudinal F-16 model developed in [8], but without thrust

vectoring. For the aerodynamic data we use the approximate data in [11], [22], with the mass and geometric properties as listed in Table I. The coefficients $C_{xq}(\alpha)$, $C_{zq}(\alpha)$, $C_{mq}(\alpha)$, $C_x(\alpha,\delta_e)$, $C_z(\alpha,\delta_e)$, and $C_m(\alpha,\delta_e)$ are taken from [11], [22], and are included in [12, Appendix A.1] in tabular form. In the simulation, the data is interpolated linearly between the points, and extrapolated beyond the table boundaries.

TABLE I

MASS AND GEOMETRIC PROPERTIES.

Parameter	Symbol	Value
Weight	W (lb)	20500
Moment of inertia	I_y (slug-ft^2)	55814
Wing area	S (ft^2)	300
Mean aerodynamic chord	$\bar{c}$ (ft)	11.32
Reference CG location	$x_{cg,ref}$	$0.35\bar{c}$

Control design for (1) is challenging because the system is highly nonlinear, and in fact, non-affine in the input. While we believe that a controller design based on an affine approximation of the form $\dot{x} = f_0(x) + g_0(x)(u + g_\delta(x,u))$ is feasible [1], we do not pursue that here, and instead adopt the more common linearization based approach. In order to perform the linearization, we make the following assumption.

Assumption 1: Given any desired equilibrium value $\hat{y} = [\hat{V}, \hat{h}]^T$, there exist a unique equilibrium input $u = \hat{u}$ and state $x = \hat{x}$, such that $f(\hat{x}, \hat{u}) = 0$.

Defining the perturbation input, state, and output respectively by $u_\delta = u - \hat{u}$, $x_\delta = x - \hat{x}$, and $y_\delta = y - \hat{y}$, we have the linear approximation $\dot{x_\delta} = Ax_\delta + Bu_\delta$, $y_\delta = Cx_\delta$, where $A = \frac{\partial f}{\partial x}(\hat{x}, \hat{u})$, $B = \frac{\partial f}{\partial u}(\hat{x}, \hat{u})$, and $C = \frac{\partial h}{\partial x}(\hat{x}, \hat{u})$. The well-known *modal decomposition* of the MIMO linearized flight dynamics into its component short-period and phugoid modes [2] yields the SISO-like state equations

$$
\begin{aligned}
\begin{bmatrix} \dot{\alpha_\delta} \\ \dot{q_\delta} \end{bmatrix} &\approx A_{11}\begin{bmatrix} \alpha_\delta \\ q_\delta \end{bmatrix} + B_{12}\,\delta_{e_\delta} \\
\begin{bmatrix} \dot{V_\delta} \\ \dot{\theta_\delta} \end{bmatrix} &\approx A_{21}\begin{bmatrix} \alpha_\delta \\ q_\delta \end{bmatrix} + A_{22}\begin{bmatrix} V_\delta \\ \theta_\delta \end{bmatrix} + B_{21}\,T_\delta + B_{22}\,\delta_{e_\delta}
\end{aligned}
\tag{2}
$$

Note that we did not include the altitude equation in (2). This is because h is not a regulated output and also does not enter the short-period and phugoid approximations (these are respectively the 2 separate sets of equations in (2)) explicitly.

We exploit the decoupling in (2) in our controller designs in the next section. In particular, we use the elevator δ_e to control the angle of attack α, and the thrust T to control the aircraft's velocity V. We emphasize that the linearization is only used in the above sense in our design, i.e., it only makes use of the decoupling in (2). Since the drag coefficients $C_i(\cdot)$ are not specified explicitly as functions of their arguments, but in tabular form (as look-up data), we use numerical techniques to both solve for the trim (equilibrium) points and

---

[1] A design for non-affine systems that partially uses the idea above can be found in [23].

[2] That such a decomposition holds for our F16 model has been verified numerically for each trim condition.

to compute the linearization. The *flight envelope* that we use for computing the trim conditions and the linearization is the cross product set $(\hat{V}, \hat{h}) \in \Omega_V \times \Omega_h$, where $\Omega_V = [300, 900]$ ft/s in steps of 100, while $\Omega_h = [5000, 40000]$ ft in steps of 5000. Both our design and the traditional gain-scheduled design are evaluated on the full fifth order nonlinear state model (1).

III. Control Design

Our primary control objective is the design of an angle of attack command system. For such a system, the entire dynamic response is important, and we assume that the desired specifications are encapsulated in a reference model. Whereas a parameter-varying reference model with higher bandwidths at higher speeds and lower bandwidths at lower speeds has been used in [4], we use a reference model with fixed parameters in our simulations. However, it is straightforward to include a parameter-varying reference model. Since the original system is MIMO, we also consider, but as a secondary objective, a Mach-hold autopilot for the regulation of the velocity V. The reference model that we use for the control of α is similar (but not identical) to the one in [4]

$$G_m(s) = \frac{\alpha_m(s)}{\alpha_d(s)} = \frac{9}{s^2 + 1.4s + 9}$$

where α_d is the angle of attack pilot command. Our approach to control design for α is based (see [17]) on minimum-phase systems transformable to the normal form $\dot{\eta} = \phi(\eta, \xi)$, $\dot{\xi} = A_c\xi + B_c\,\gamma(x)\,[u - \alpha(x)]$, $y = C_c\xi$, where $x \in R^n$ is the state, u the input, ρ is the system's relative degree, $\xi \in R^\rho$ the output and its derivatives up to order $\rho - 1$, $\eta \in R^{n-\rho}$ the part of the state corresponding to the internal dynamics, and the triple (A_c, B_c, C_c) a canonical form representation of a chain of ρ integrators. A SMC design for such a system was carried out in [17], with the assumption that the internal dynamics $\dot{\eta} = \phi(\eta, \xi)$ are input-to-state stable (ISS) with ξ as the driving input. For such systems, it is shown in [17] that a continuous sliding mode controller of the form

$$u = -k\,\mathrm{sign}(\gamma(x))\,\mathrm{sat}\left(\frac{k_0\sigma + k_1e_1 + k_2e_2 + \cdots + e_\rho}{\mu}\right)$$
$$(3)$$

can be designed to achieve robust regulation, where e_1, ..., e_ρ are the tracking error and its derivatives up to order ρ, the positive constants $k_i, i = 1, \cdots, \rho - 1$ in the sliding surface function

$$s = k_0\sigma + \sum_{i=1}^{\rho} k_ie_i + e_\rho \qquad (4)$$

are chosen such that the polynomial $\lambda^{\rho-1} + k_{\rho-1}\lambda^{\rho-2} + \cdots + k_1$ is Hurwitz, and σ_i is the output of the "conditional integrator"

$$\dot{\sigma} = -k_0\sigma + \mu\,\mathrm{sat}\left(\frac{s}{\mu}\right), \;\; \sigma(0) \in [-\mu/k_0, \mu/k_0] \qquad (5)$$

where $k_0 > 0$, and $\mu > 0$ is the "width" of the boundary layer. From (4) and (5), it is clear that inside the boundary

layer $|s| \leq \mu$, $\dot{\sigma} = k_1e_1 + k_2e_2 + \cdots + e_\rho$, which implies that $e_i = 0$ at equilibrium, i.e., (5) is the equation of an integrator that provides integral action "conditionally", inside the boundary layer. As shown in [17], such a design provides asymptotic error regulation, while not degrading the transient performance, as is common in a conventional design that uses the integrator $\dot{\sigma} = e_1$. In the case of relative degree $\rho = 1$ and $\rho = 2$, the controller (3) is simply a specially tuned saturated PI/PID controller with anti-windup (see [17, Section 6]).

The control (3) can be extended to the output-feedback case by replacing e_i by its estimate $\hat{e}_i$, obtained using the high-gain observer (HGO)

$$\left.\begin{array}{rcl} \dot{\hat{e}}_i &=& \hat{e}_{i+1} + \alpha_i(e_1 - \hat{e}_1)/\epsilon^i, \; 1 \leq i \leq \rho - 1 \\ \dot{\hat{e}}_\rho &=& \alpha_\rho(e_1 - \hat{e}_1)/\epsilon^\rho \end{array}\right\} \quad (6)$$

where $\epsilon > 0$, and the positive constants α_i are chosen such that the roots of $\lambda^\rho + \alpha_1\lambda^{\rho-1} + \cdots + \alpha_{\rho-1}\lambda + \alpha_\rho = 0$ have negative real parts. To complete the design, we need to specify how k, μ and ϵ (in the output-feedback case) are chosen. The parameter k is chosen "sufficiently large" (to overbound uncanceled terms in $\dot{s}$) while μ and ϵ are chosen "sufficiently small", the former to recover the performance of ideal (discontinuous) SMC (without an integrator) and the latter to recover the performance under state-feedback with the continuous SMC. Analytical results for stability and performance are given in [17], but are not directly applicable to this work since they were done for control affine systems. Consequently, we only apply the design to the (control affine) linear approximation (2) and "verify" the efficacy of the design through simulations. A mention of stability and boundedness under this design is made in the concluding paragraph of this section.

A. The relative degree $\rho = 1$ case

In order to formally apply the controller design to the short period approximation in (2), with δ_{e_δ} as input and α_δ as output, we need to compute this system's relative degree, transform it to normal form and check internal stability. The next assumption states these properties.

Assumption 2: Consider the short-period approximation

$$\begin{bmatrix} \dot{\alpha}_\delta \\ \dot{q}_\delta \end{bmatrix} \overset{\mathrm{def}}{=} \begin{bmatrix} a_{\alpha\alpha} & a_{\alpha q} \\ a_{q\alpha} & a_{qq} \end{bmatrix}\begin{bmatrix} \alpha_\delta \\ q_\delta \end{bmatrix} + \begin{bmatrix} b_{\alpha\delta} \\ b_{q\delta} \end{bmatrix}\delta_{e_\delta}$$

with output α_δ. Then (i) $b_{\alpha\delta} < 0$, so that the relative degree $\rho = 1$, and (ii) $A_{11} = \begin{bmatrix} a_{\alpha\alpha} & a_{\alpha q} \\ a_{q\alpha} & a_{qq} \end{bmatrix}$ is Hurwitz, i.e., the system is minimum-phase.

While we have only verified Assumption 2 numerically, for each trim condition, an analytic discussion based on the stability derivatives can be found in [22]. Assumption 2 allows us to design a SMC controller of the form (3) for the α-dynamics. Because of the integrator, we don't need to add a (gain-scheduled) nominal value to our perturbation input, i.e., we can simply take the output of the controller (3) to be u, not u_δ. In particular, since $\rho = 1$, and the high-frequency gain $b_{\alpha\delta} < 0$, the control (3) specializes to the

saturated PI controller

$$\delta_e = k \, \text{sat}(s/\mu) = k \, \text{sat}\left(\frac{k_0\sigma + e}{\mu}\right) \quad (7)$$

with $\dot{\sigma} = -k_0\sigma + \mu \, \text{sat}\left(\frac{k_0\sigma+e}{\mu}\right)$ where $e = \alpha - \alpha_m$, $k_0, \mu > 0$, and $k > 0$ is simply chosen to be the maximum allowable limit for δ_e. This completes the design of the controller.

B. The relative degree $\rho = 2$ case

While in Assumption 2(i), we said $b_{\alpha\delta} < 0$, it is seen (numerically) that $b_{\alpha\delta} \approx 0$ (this is not simply a "scaling" issue, as $|b_{\alpha\delta}| \ll |b_{q\delta}|$). Consequently, the short period approximation (2) with output α_δ is "practically" relative degree $\rho = 2$ [3] and not $\rho = 1$, so that the control (3) now becomes that of a saturated PID controller

$$u = k \, \text{sat}(s/\mu) = k \, \text{sat}\left(\frac{k_0\sigma + k_1 e + \dot{e}}{\mu}\right) \quad (8)$$

with $k_0, k_1, \mu > 0$, and as before $k > 0$ simply chosen to be the maximum allowable limit for δ_e. The expression for the control involves the derivative of α, and it well-known that the measurement of α is often noisy because of turbulence. For example, it is common (see, for example, [22]) to assume measurements of α to be corrupted by vertical wind gust noise w_g, with spectral density given by the *Dryden model*, and generated (approximately) by the controllable canonical realization of the shaping filter

$$\dot{z} = A_w z + B_w w, \ w_g = C_w z \quad (9)$$

driven by the white noise input $w(t) \sim (0,1)$. For our purposes, we simply assume that the derivative $\dot{e}$ in (8) is unavailable as a direct measurement and use the HGO (6) to estimate it (in fact, in simulations with noise, we also replace e by its estimate $\hat{e}$ obtained from the HGO). A discussion of the effect of measurement noise on the HGO is discussed in [2], under the assumption that the noise signal is the output of a linear system driven by a bounded input, which is the case here.

Since we are only interested in the Mach-hold autopilot (for V) as a secondary objective (of minor importance), and this is usually designed simply to meet specifications on steady-state error and disturbance rejection, we only design a simple PI controller for the thrust T to regulate V. The V_δ-dynamics in (2) are of the form

$$\dot{V}_\delta \overset{\text{def}}{=} a_{V\alpha}\alpha_\delta + a_{Vq}q_\delta + a_{VV}V_\delta + a_{V\theta}\theta_\delta + b_{VT}T_\delta + b_{V\delta}\delta_{e_\delta}$$

and it can be verified that for each trim condition, $a_{VV} < 0$, i.e., the V_δ-subsystem is stable. We view the term $a_{V\alpha}\alpha_\delta + a_{Vq}q_\delta + a_{V\theta}\theta_\delta + b_{V\delta}\delta_{e_\delta}$ as constituting a "matched disturbance", and simply "augment" the stability of this system by designing T_δ as the PI controller

$$T_\delta = -k_P V_\delta - k_I \sigma_V, \ \dot{\sigma}_V = V_\delta \quad (10)$$

with the gains $k_p, k_I > 0$ chosen to assign the eigenvalues of the resulting 2nd-order system (with states σ_V and V_δ) at desired pole locations.

As previously mentioned, the analytical results of [17] do not directly apply to this design, and we do not provide a rigorous analysis here. However, assuming that the short-period approximation holds, a naive argument that the controller achieves boundedness of all states, and asymptotic error regulation of the error e is presented below. The SMC (7) achieves robust regulation of the angle of attack α, provided the value of k is "sufficiently large". The variable q is bounded since the system is minimum-phase. The variable θ evolves according to $\dot{\theta} = q$, and hence is bounded whenever q is. The PI controller (10) achieves boundedness of the velocity V. Finally, from the equation of $\dot{h}$, it follows that h is bounded for all finite time whenever V is, so that with our SMC and PI controllers for δ_e and T respectively, all the states of the closed-loop system are bounded. Our simulation results, which we present next, appear to validate the above conclusions.

IV. Simulation Results

Numerical values of the SMC parameters that we use in all the simulations are $k_0 = k_1 = 1$, and that $k = 25$, so that $-25 \leq \delta_e \leq 25$, also used in [15]. The initial values in all simulations correspond to trim conditions with $(\hat{V}, \hat{h}) = (600ft/s, 20000ft)$. The control is always tested on the full 5th order nonlinear model. While we did compare our simulation results against a more classical gain-scheduled polynomial-based approach to model following (described in [12, Chapter 3]), they are not presented here, and we only mention that the SMC design in this paper far outperforms the gain-scheduled design.

Our first simulation shows the performance with no integral action and assuming $\rho = 1$, i.e., $u = -k \, \text{sat}\left(\frac{e_1}{\mu}\right)$, with $\mu = 0.1$, when the pilot command α_d is a doublet-like signal with value 15 for $0 \leq t < 5$, -5 deg for $5 \leq t < 10$ and 0 for $t \geq 10$. The results are shown in Figure 1, and we see that the controller achieves good performance, in spite of reaching the saturation limits, and even without integral control. In particular, the relative error is less than 0.4% when the control is not saturated and roughly 8% for the brief period when the control is saturated [4].

In order to demonstrate the performance of the robustness of the SMC approach to matched disturbances, and the effect of integral action on the steady-state performance, we repeat the first simulation, but with an input additive disturbance at the elevator input. Note that this disturbance effectively replaces δ_e in every equation in (1) by $\delta_e + d$. Figure 2 shows the simulation results for $d = -5$, both without integral control, and with the conditional integrator, and for the values $\mu = 0.5$ and $\mu = 0.1$. The following inferences can be made (i) the transient responses of the controllers are good, even with the disturbance d, with a maximum absolute error of

---

[3]This assumption corresponds to the observation that the lift derivative is small with respect to the velocity V and can hence be neglected, and is made in [23] right from the start.

[4]By comparison, $\max|e| \approx 25\%$ with the gain-scheduled polynomial approach with integral control *even when the control is not saturated*.
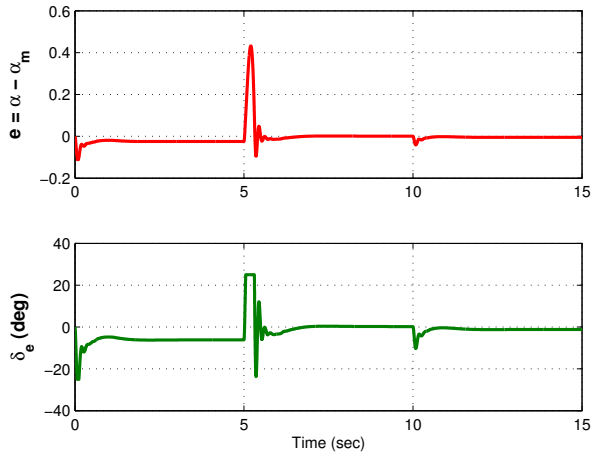
Fig. 1. Tracking errors with SMC without integral control, $\mu = 0.1$.

approximately 0.04 (or a relative error of 0.8%) even without integral control and with a value of μ as large as 0.5, (ii) the steady-state error is non-zero without integral control, and (approximately) zero with integral control. In particular, in the absence of integral control, $|e| = O(\mu)$, and we must decrease μ in order to achieve smaller steady-steady state errors, and this is clear from the simulation results. However, smaller values of μ can induce chattering when there are switching imperfections such as delays, and has been demonstrated by simulations for the case of pitch-rate control of the same F-16 model as the one in this paper in [13]. On the other hand, the inclusion of integral action means that we don't need to make μ very small to achieve small errors, only small enough to stabilize the equilibrium point.
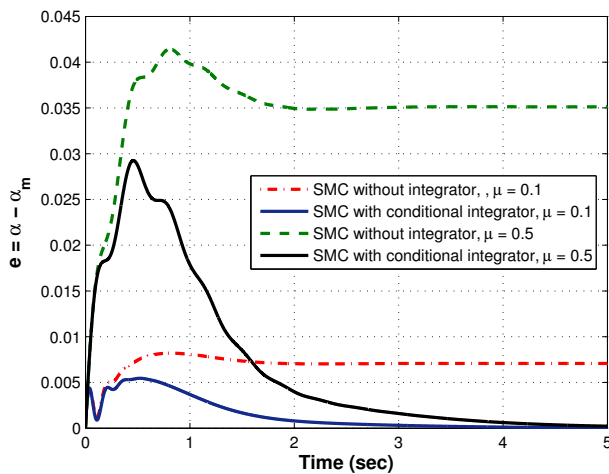

Fig. 2. Tracking errors with input-additive disturbance, with and without integral control, $\mu = 0.1, 0.5$.

Next, we compare the control designs for the $\rho = 1$ and $\rho = 2$ cases, with $\mu = 0.1$, and for a reference doublet of magnitude 5 deg. We assume that the measurement of

α is not corrupted by noise, and use the HGO to estimate the derivative $\dot{e}$ required in the $\rho = 2$ case. The values of the HGO parameters are taken as $\alpha_1 = 15$, $\alpha_2 = 50$, and $\epsilon = 0.01$. The simulation results are shown in Figure 3 (we have plotted the results at the times when the input doublet changes values), and some interesting observations can be made: (i) the error is much smaller for the controller designed under the assumption that $\rho = 2$, and moreover, (ii) the control magnitude is smaller and "smoother" with $\rho = 2$ than for $\rho = 1$. We believe this is because of the small magnitude of the high-frequency gain with $\rho = 1$, which renders the control less effective than with the assumption $\rho = 2$.
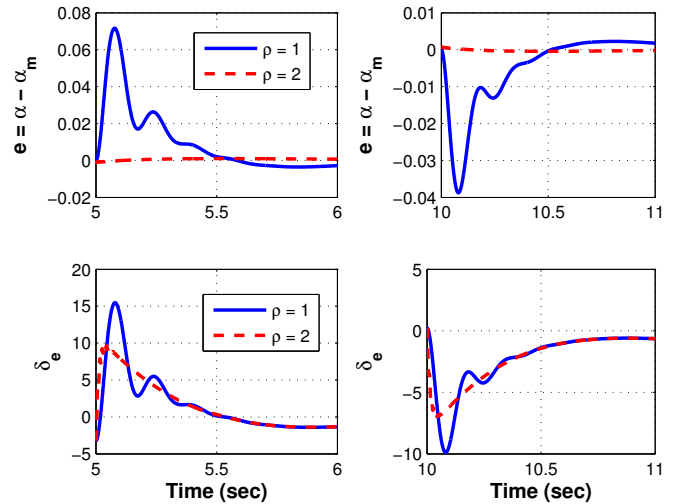

Fig. 3. Effect of relative degree assumption: tracking errors with controller designs for $\rho = 1$ and $\rho = 2$.

In order to demonstrate the effect of measurement noise on the HGO, we repeat the previous simulation with α corrupted by measurement noise, for $\rho = 1$ and $u = k\text{sat}\left(\frac{k_0\sigma + e}{\mu}\right)$, and with $\rho = 2$ and $u = k\text{sat}\left(\frac{k_0\sigma + k_1\hat{e} + \hat{\dot{e}}}{\mu}\right)$. We use the noise model (9) with fixed coefficient matrices [5] (see [22]) $A_w = \begin{bmatrix} 0 & 1 \\ -0.0823 & -0.5737 \end{bmatrix}$, $B_w = \begin{bmatrix} 0 \\ 1 \end{bmatrix}$, $C_w = [0.0043 \ 0.0262]$. The simulation results in Figure 4 clearly show that (i) the presence of noise does not degrade the derivative estimate, and in fact, as before (ii) the design with $\rho = 2$ (that uses the derivative estimate from the HGO) is marginally better (note the error at $t = 5$ and $t = 10$, when the doublet changes in value) than the (differentiation-free) $\rho = 1$ based design.

Lastly, before we summarize our results, we present our results for velocity tracking with the PI controller, with gains $k_P = 828.4$ and $k_I = 191.2$ chosen to assign the roots of the closed-loop characteristic polynomial $\lambda^2 + b_{VT}k_P\lambda + b_{VT}k_I$ at -0.3 and -1. The desired velocity reference is the output of the first order filter $H(s) = \frac{1}{s+1}$, to which the input is a

[5]This is not really an accurate wind turbulence model, since the matrices depend on velocity, altitude and atmospheric conditions. Our goal is to simply include *a* noise model.
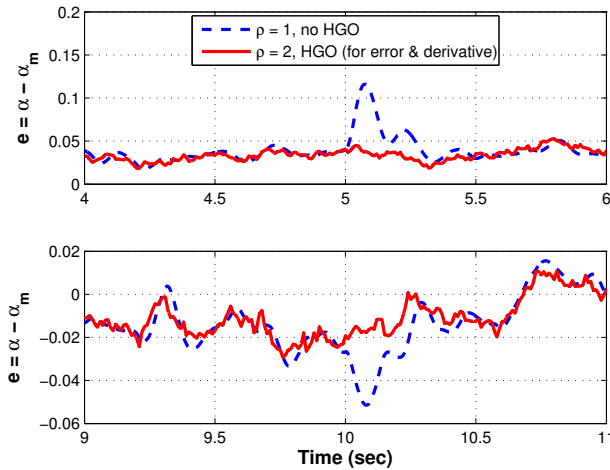
Fig. 4.   Effect of measurement noise on output feedback using the HGO.

doublet-like signal with an initial value of 600 ft/s, changing to 500 ft/s at $t = 17s$, and to 700 ft/s at $t = 35s$. The results are shown in Figure 5, and it is clear that this simple controller achieve robust regulation, even though its transient performance is not very good, as expected. We can improve the design of the velocity controller using techniques like SMC or other robust linear techniques, but do not pursue it, since velocity control is only a secondary objective.
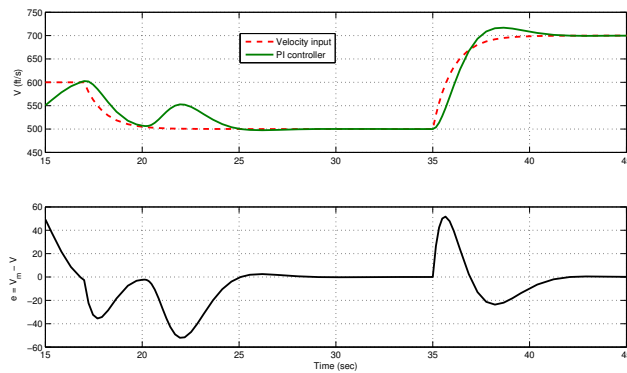

Fig. 5.   Velocity (Mach-hold) autopilot response to velocity command: PI controller.

V. CONCLUSIONS

We have presented a new SMC design for control of the angle of attack of an F-16 aircraft, based on the conditional integrator design of [17]. The design exploits the short-period approximation of the linearized flight dynamics. The robustness of the method to disturbances, modeling uncertainties and measurement noise was demonstrated through simulation, with the method outperforming, without any scheduling, the transient and steady-state performance of a conventional gain-scheduled model-following controller. The method is also applicable to control of the pitch-rate. While we did not present any analytical results, we believe, that

analytical results based on a control-affine approximation of the nonlinear system should be possible. Consequently, we believe that the results presented in this paper are a promising start to demonstrate the efficacy of the conditional integrator based SMC design to flight control.

REFERENCES

[1] R.J. Adams, J.M. Buffington, and S.S Banda. Design of nonlinear control laws for high-angle-of-attack flight. *Jnl. Guidance, Control, and Dynamics*, 17(4):737–745, 1994.

[2] J.H. Ahrens and H.K. Khalil. Output feedback control using high-gain observers in the presence of measurement noise. In *Proc. 2004 Amer. Ctrl. Conf.*, 2004.

[3] G.J. Balas.   Flight control law design: An industry perspective. *European Jnl. of Ctrl.*, 9(2-3):207–226, 2003.

[4] J.M. Biannic and P. Apkarian. Parameter varying control of a high performance aircraft.   In *Proc. AIAA, Guidance, Navigation and Control Conference*, pages 69–87, 1996.

[5] Y.J. Huang, T.C. Kuo, and H.K. Way. Robust vertical takeoff and landing aircraft control via integral sliding mode. *Control Theory and Applications, IEE Proceedings-*, 150:383–388, 2003.

[6] E.M. Jafarov and R. Tasaltin.   Robust sliding-mode control for the uncertain MIMO aircraft model F-18. *IEEE Trans. Aerospace Electronic Sys.*, 36(4):1127–1141, 2000.

[7] T. Lee and Y. Kim. Nonlinear adaptive flight control using backstepping and neural networks controller. *Jnl. Guidance, Control, and Dynamics*, 24(4):675–682, 2001.

[8] B. Lu. *Linear Parameter-Varying Control of an F-16 Aircraft at High Angle of Attack*. PhD thesis, North Carolina State University, 2004.

[9] B. Lu, F. Wu, and S. Kim. LPV antiwindup compensation for enhanced flight control performance. *Jnl. Guidance, Control and Dynamics*, 28:495–505, 2005.

[10] J-F. Magni, S. Bennani, and J. Terlouw (Eds). *Robust Flight Control: A Design Challenge*. Lecture Notes in Control and Information Sciences - Vol 224. Springer, 1998.

[11] L.T. Nguyen, M.E. Ogburn, W.P. Gillert, K.S. Kibler, P.W. Brown, and P.L. Deal. Simulator study of stall/post-stall characteristics of a fighter airplane with relaxed longitudinal static stability. *NASA Technical Paper 1538*, 1979.

[12] E. Promtun. *Sliding Mode Control of F-16 Longitudinal Dynamics*. MS. Thesis, San Diego State University, San Diego, USA, 2007.

[13] E. Promtun and S. Seshagiri. Sliding mode control of pitch-rate of an f-16 aircraft (submitted). In *17th IFAC World Congress*, Seoul, S. Korea, July 2008.

[14] W.C. Reigelsperger and S.S. Banda.   Nonlinear simulation of a modified F-16 with full-envelope control laws. *Control Engineering Practice*, 6:309–320, 1998.

[15] Richard S. Russell. Non-linear F-16 simulation using Simulink and Matlab. Technical report, University of Minnesota, June 2003.

[16] R. Rysdyk and A.J. Calise. Robust nonlinear adaptive flight control for consistent handling qualities. *IEEE Trans. Aut. Ctrl.*, 13(6):896–910, 2005.

[17] S. Seshagiri and H.K. Khalil.   Robust output feedback regulation of minimum-phase nonlinear systems using conditional integrators. *Automatica*, 41(1):43–54, 2005.

[18] J.S. Shamma and J.S. Cloutier. Gain-scheduled bank-to-turn autopilot design using linear parameter varying transformations. *Jnl. Guidance Control and Dynamics*, 9(5):1056–1063, 1996.

[19] Y. Shtessel, J. Buffington, and S. Banda. Tailless aircraft flight control using multiple time scale reconfigurable sliding modes. *IEEE Trans. Ctrl. Sys. Tech.*, 10(2):288–62, 2002.

[20] S.A. Snell, D.F. Enns, and Jr. W.L. Garrard. Nonlinear inversion flight control for a supermaneuverable aircraft. *Jnl. Guidance, Control, and Dynamics*, 15(4):976–984, 1992.

[21] M.S. Spillman. Robust longitudinal flight control design using linear parameter-varying feedback. *Jnl. Guidance, Control, and Dynamics*, 23(1):101–108, 2000.

[22] B.L. Stevens and F.L. Lewis. *Aircraft Control and Simulation*. John Wiley & Sons, Inc., 2 edition, 2003.

[23] A. Young, C. Cao, N. Hovakimyan, and E. Lavretsky. An adaptive approach to nonaffine control design for aircraft applications. In *AIAA Guidance, Navigation, and Control Conference and Exhibit*, Keystone, CO, USA, August 2006.